PHYSICS-BASED MODELING OF NPT AND PT IGBTS AT DEEP CRYOGENIC TEMPERATURES

A. Caiafa, A. Snezhko*, J.L. Hudgins†, E. Santi, R. Prozorov*, and P.R. Palmer‡**
Department of Electrical Engineering
University of South Carolina
Columbia, SC 29208, USA
caiafaa@engr.sc.edu

*Department of Physics and Astronomy
University of South Carolina
Columbia, SC 29208, USA

† Department of Electrical Engineering
University of Nebraska
Lincoln, NE 68588-0511 USA

‡ Department of Engineering
University of Cambridge
Trumpington Street
Cambridge CB2 1PZ, UK

***Abstract* - Detailed experimental data taken for punch-through (PT) and non-punch-through (NPT) Insulated Gate Bipolar Transistors (IGBTs) are presented. The test program covered IGBT devices rated for 100–600 A and 600-1200 V from different manufacturers. The turn off behavior of the IGBTs is examined over a temperature range of 4.2 to 295 K. Physical behavior at low junction temperatures is analyzed. The IGBTs are consequently modeled using the Palmer-Leturcq model, a physics-based model based on the Fourier expansion of the ambipolar diffusion equation.**

I. INTRODUCTION

In recent years, there has been an increasing interest in semiconductor device behavior at low temperatures. While the behavior of power electronics devices down to a liquid nitrogen temperature of 77 K, (LNT) has been explored [1-2], there are just a few studies related to the behavior of power electronics devices at a liquid helium temperature of 4.2 K, (LHT) [3], a study on thyristors [4], and very limited data on Insulated Gate Bipolar Transistors (IGBTs) [5-6]. The interest in the behavior of power electronic devices at cryogenic temperatures lower than LNT originates from the possible application of semiconductor switches in conjunction with superconductor materials operating at a high energy level. Examples of the application of such superconductor technology are SMES (Superconducting Magnetic Energy Storage System) [4], [5], [7], MAGLEV train technology (Japanese solution), and, more recently, a superconducting transformer developed and installed by ABB in 1997, and 100 MW superconducting cables installed by Pirelli in 2001 for Detroit Edison. Due to extreme temperatures of the outer planets of the solar system, the USA space program (NASA) is also interested in this particular topic. Being able to switch large amounts of power in a short time, the IGBT seems to be a particularly well-suited device for these applications. This paper is part of a larger study and will address the turn-off behavior of Punch-Through (PT) and Non-Punch-Through (NPT) IGBTs at very low temperatures. Modeling of their behavior using the Palmer-Leturcq model is performed. This paper discusses losses during the turn off at cryogenic temperatures.

II. EXPERIMENTAL SET-UP

The experimental setup is designed in order to capture the switching behavior of the Device Under Test (DUT). The main goals pursued in designing the test bed are to minimize the overall parasitic inductance, to provide cooling of the DUT only, and to give an easy way to modify the load impedance. Details concerning these issues are addressed in the main work [8].

The structure of the experimental setup includes a set of five capacitors connected in parallel, one isolated dc voltage source, two isolated small voltage sources, one gate drive, one isolated logic double-pulse generator, one cryostat, and one vacuum pump station. The layout of the circuit is shown in Figure 1 and the electrical circuit, inclusive of parasitic elements, is shown in Figure 2.

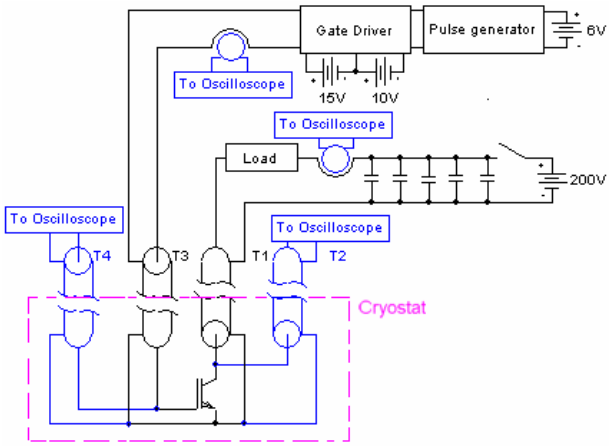

Figure 1: Experimental setup.

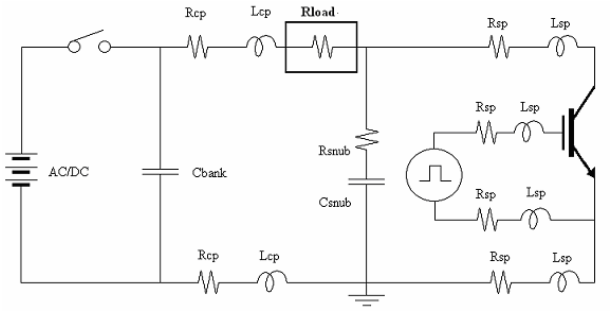

Figure 2: Electrical circuit inclusive of parasitic elements

As it is illustrated in Figure 1, the voltages are measured using the four-point probe technique, a requirement imposed by the presence of the stainless steel pipes T1-T4, which add non-negligible parasitic resistances R_{sp} and parasitic inductances L_{sp}. Due to the presence of the stainless steel pipes, particular consideration has been given to the grounding of the system and of all the instrumentation used. In the experimental setup the device current was measured at resistor R_{load} location and therefore it includes the snubber current as well. As a result, all reported IGBT current waveforms include the snubber current, with the exception of Figure 7 and Figure 8, which are previous results, and Figure 13 and Figure 14, where the actual IGBT current was numerically reconstructed from the load current and the IGBT collector-emitter voltage.

The temperature was measured by a Lakeshore silicon diode probe that was attached to the package base plate of the DUT. The DUT is cooled slowly over a period of about two days. The refrigerating procedure will be explained in detail in the final document. During the measurements, the thermal system is "open", meaning that the vaporized helium inside the cryostat flows to the outside environment, a condition that allows easier adjustment of the DUT temperature. The tested devices are listed in Table 1. The DUTs have been tested with three differend resistive loads and one clamped inductive load.

Once the DUT is at liquid helium temperature (LHT), the bank capacitor is charged to 200 V. The DUT is pulsed twice: first it is turned on for 10 µs, then off for 20 µs, then on again for 10 µs. Once the DUT is tested with all different loads at LHT, the liquid helium flow is cut causing the junction temperature of the DUT to slowly increase. The testing is repeated at several temperatures. Once the temperature is in the vicinity of 70 K, the DUT is submerged with liquid nitrogen. This ensures that the DUT temperature stays constant at LNT. .

III. Experimental Results

Experimental testing of six IGBTs has been performed using the experimental set-up shown in Figure 1 corresponding to the schematic shown in Figure 2. The main characteristics of the six Devices Under Test (DUTs) are listed in Table 1.

Name	Gate Configuration	Structure	I_{cmax} (A)	V_{ces} (V)
a	Planar	NPT	600	1200
b	Trench	PT	600	1200
c	Trench	PT	600	600
d	Planar	PT	100	600
e	Planar	PT	100	600
f	Planar	NPT	100	600

Table 1: Tested Devices and Ratings

Some experimental results such as conduction losses, turn-off time, forward voltage drop characteristics, and switching losses have already been presented in [8]. This section presents and discusses data relative to state diagram of the IGBTs (both PT and NPT), for temperatures ranging from 300 K to 4.2 K. Figure 3 shows the state diagram of a NPT planar gate IGBT rated for 100 A and 600 V during resistive turn-off from a peak collector current of approximately 100 A, at various temperatures. It is noticeable how the device has increased overshoot at lower temperatures. This can limit its use at low temperatures due to the SOA of the device. It is clear that stray inductance in the main current path dominates the behavior at low temperatures because of the faster IGBT turn-off as shown in Figure 4.

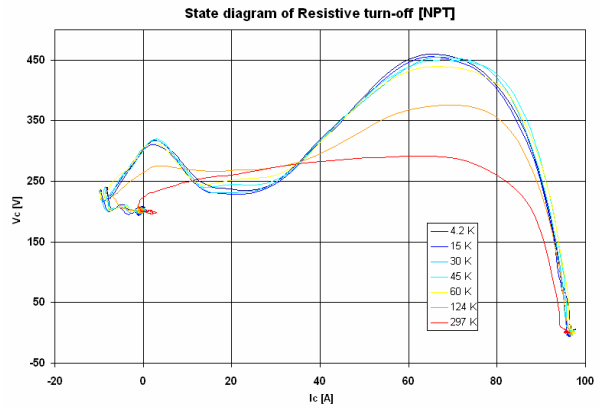

Figure 3: State diagram of a NPT planar gate IGBT rated for 100 A and 600V (device *f*). Current waveforms include snubber current.

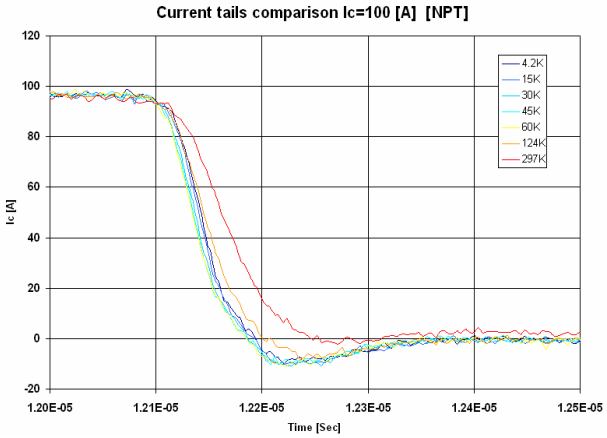

Figure 4: Turn off current waveforms of a NPT planar gate IGBT rated for 100 A and 600 V (device *f*). Current waveforms include snubber current.

From Figure 4 it can be observed that the current fall time exhibits a significant decrease as temperature decreases from 297 to 60 K and then exhibits a modest increase as temperature decreases from 45 to 4.2 K. The reduction in transition time for operating temperatures of 297 to 60 K can be attributed to an increase in the charge carrier mobility and a decrease in the charge carrier lifetime. The increase in transition times observed at very low temperatures (45 to 4.2 K curves) can be attributed to a leveling of electron mobility value at around 20 K and to a slight decrease in mobility value below 10 K as indicated by data [6], [8], [9], and [10]. This is to be expected as impurity scattering mechanisms, at the lowest temperatures, begin to dominate over the meager lattice scattering in this extreme operating regime.

While all the other tested samples listed in Table 1 exhibit a behavior similar to the one reported in Figure 3 and Figure 4, sample *e* exhibits an increasing turn off time as the temperature decreases as Figure 5 shows. As a result, the greatest overshoot appears at higher temperatures (Figure 6).

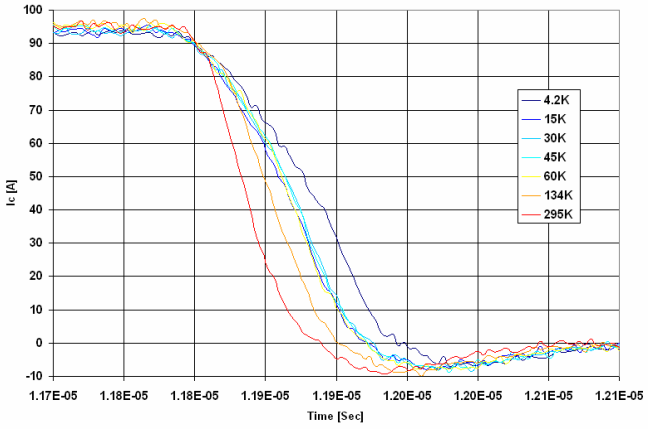

Figure 5: Turn off waveforms of a PT planar gate IGBT rated for 100 A and 600 V (device *e*). Current waveforms include snubber current.

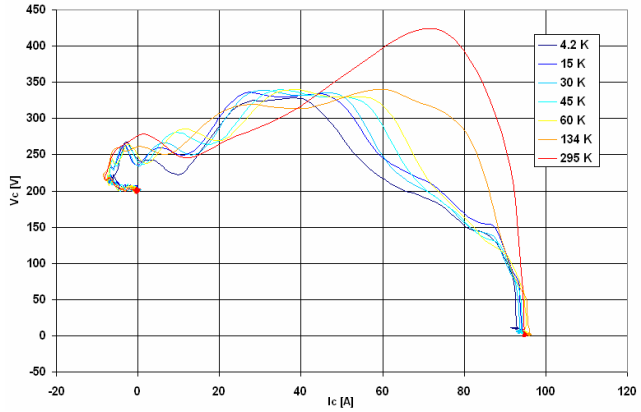

Figure 6: State diagram of a PT planar gate IGBT rated for 100 A and 600V (device *e*). Current waveforms include snubber current.

IV. IGBT Physics-Based Model with Temperature Dependencies

The behavior of conductivity-modulated devices, such as diodes and IGBTs, depends heavily on the excess carrier (charge) distribution in the wide drift region. In modern IGBTs, the charge profile has a 1D form over about 90% of its volume [11]. Thus, a 1D solution is adequate for the bulk of the device. Space-charge neutrality is maintained with the majority carrier profile closely matching the minority carrier profile (quasi-neutrality). Under these conditions, assuming high-level injection, the charge dynamics are described by the ambipolar diffusion equation:

$$D \cdot \frac{\partial^2 \delta p(x,t)}{\partial x^2} = \frac{\delta p(x,t)}{\tau_{HL}} + \frac{\partial \delta p(x,t)}{\partial t} \qquad (1)$$

where D is the ambipolar diffusion coefficient, τ_{HL} is the high-level carrier lifetime within the drift region and $p(x,t)$ is the excess carrier concentration. A solution for this equation was proposed for diodes [12], and extended for IGBTs [11]. The main feature of this model is that the solution of equation (1) is based on the Fourier expansion of the charge distribution according to equation (2).

$$\delta p(x,t) = \delta p_o(t) + \sum_{k=1}^{\infty} \delta p_k(t) \cdot \cos\left(\frac{k \cdot \pi \cdot (x - x_1)}{x_2 - x_1}\right) \qquad (2)$$

Equation (2) has been implemented into PSpice™ using an RC-network.

The IGBT model used in this work implements this approach for the representation of the drift region. The model contains details of the MOS gate, the depletion layer capacitances, and the buffer layer (for punch-through devices). Moreover, the model includes the temperature dependencies of parameters such as carrier lifetime, mobilities, intrinsic carrier concentration, MOS threshold voltage, and transconductance, so it can correctly reproduce the changes in device behavior as a function of temperature. The model has been verified through experimental testing of diodes, and PT and NPT IGBTs with both planar and trench-gate structures, over a temperature range from –150 to 150 °C [11], [13], [14], and [15]. Some typical turn-off waveforms comparing model predictions and experimental results are shown in Figure 7 and Figure 8 for PT and NPT devices respectively. The results clearly show the validity of the model in the temperature range described.

The waveforms shown in Figure 7 and Figure 8 are for a 600 V, 600 A trench-gate punch-through (PT) IGBT and for a similar NPT device.

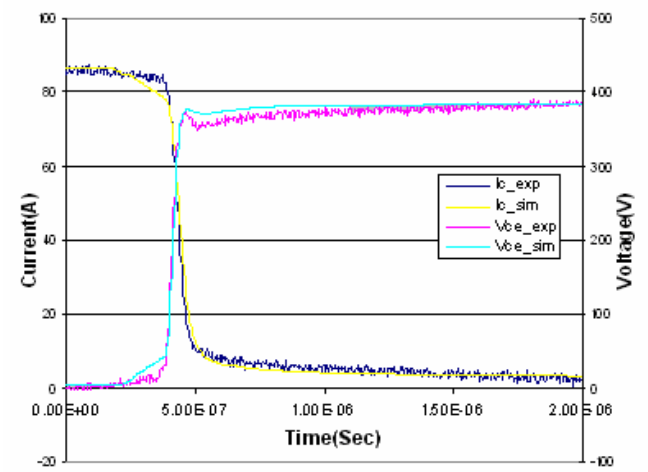

Figure 7: Collector current fall and voltage rise of NPT during turn-off at temperatures of –125 °C. The simulated waveforms are blue (voltage) and yellow (current).

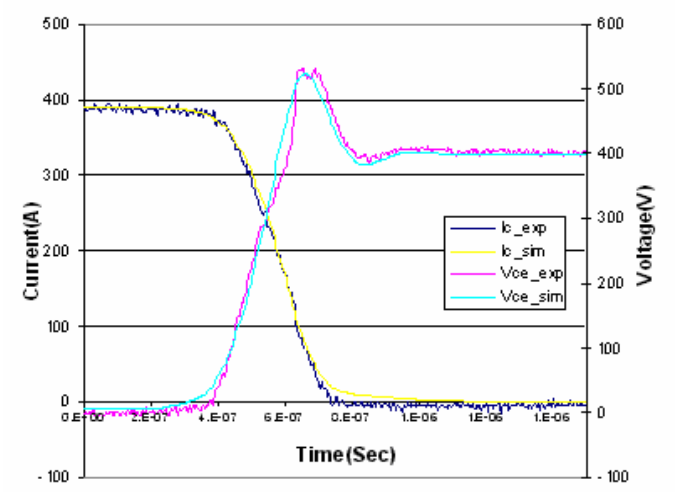

Figure 8: Collector current fall and voltage rise of PT-IGBT during turn-off at temperatures of 100 °C. The simulated waveforms are blue (voltage) and yellow (current).

V. Comparison of Experimental and Simulation Results

Figure 9 to Figure 14 show the simulation results compared with the experimental data for a Punch-Through trench-gate device rated for 600 A and 600 V (device *c* of Table 1). The device was tested under 2 Ω resistive switching condition. The Palmer-Leturcq IGBT model described in [14] has been modified to extend its validity to deep cryogenic temperatures. In particular, the temperature dependencies for silicon parameters proposed by the authors in [6] have been implemented in the model. The parasitics associated with the experimental set-up have also been included as lumped elements in the simulation circuit (equivalent circuit shown in Figure 2).

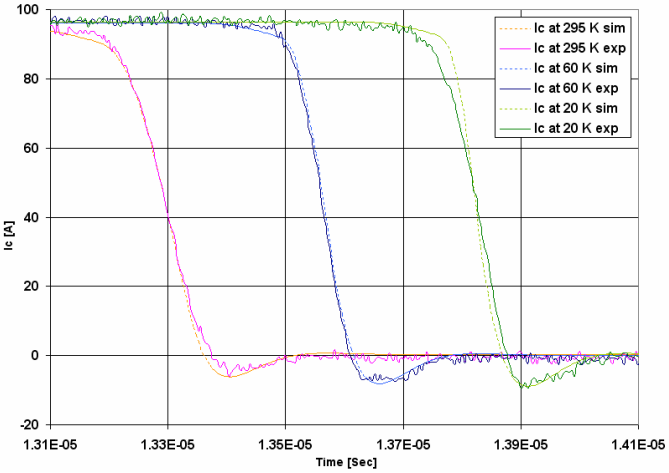

Figure 9: Family of curves of simulated and experimental current Ic at 295 K, 60 K and 20 K. Current waveforms include snubber current.

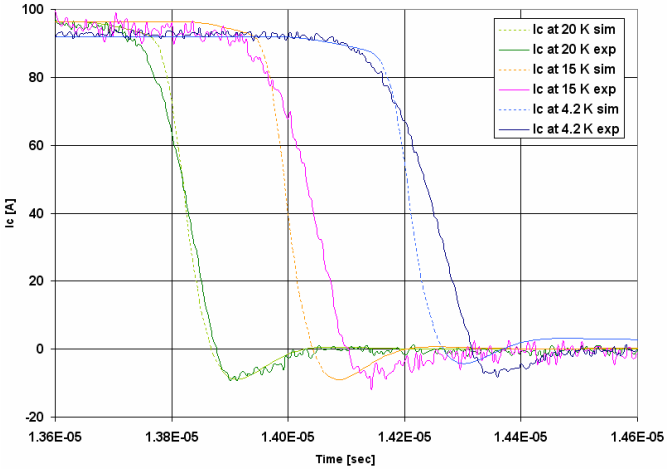

Figure 10: Family of curves of simulated and experimental current Ic at 20 K, 15 K and 4.2 K. Current waveforms include snubber current

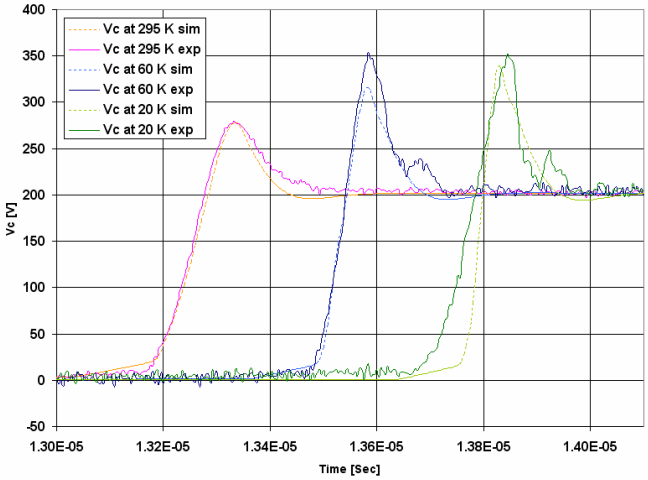

Figure 11: Family of curves of simulated and experimental collector-emitter voltage Vc at 295 K, 60 K and 20 K.

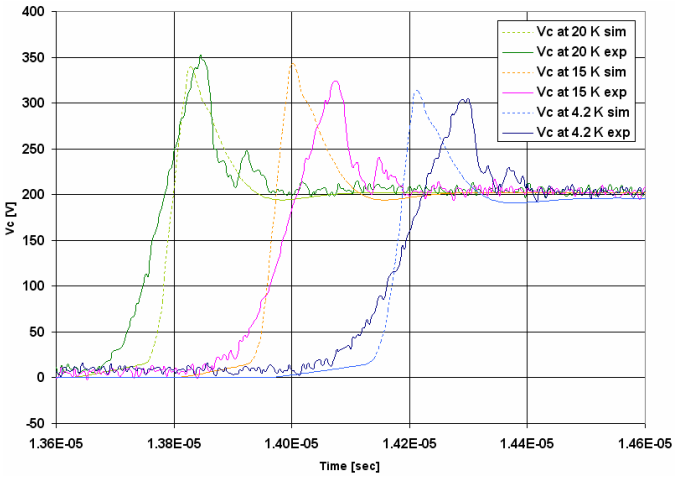

Figure 12: Family of curves of simulated and experimental collector-emitter voltage Vc at 20 K, 15 K and 4.2 K.

Figure 9 and Figure 10 show a family of curves for the simulated and experimental IGBT currents over a wide range of temperatures. The simulated and experimental data match fairly well from room temperature to 20 K. At 20 K the simulated current fall time is slightly faster than the experimental current fall time. The discrepancy becomes more significant as the temperature decreases. Figure 11 and Figure 12 show the corresponding family of curves for collector-emitter voltage. The data show the same trends observed for the collector currents. There is good matching above 20 K, but the simulation results give a faster voltage rise time below 20 K. The discrepancy between simulation and experiment for the collector-emitter voltage is more evident than for the collector current, because the voltage waveform is more affected by the presence of parasitic circuit elements. The higher peaks of the simulated waveforms observed at very low temperatures are associated with the faster transition times. It must be noted that the simulated voltage waveforms corresponding to a junction temperature lower than 20 K do not capture the high forward voltage drop observed experimentally [8].

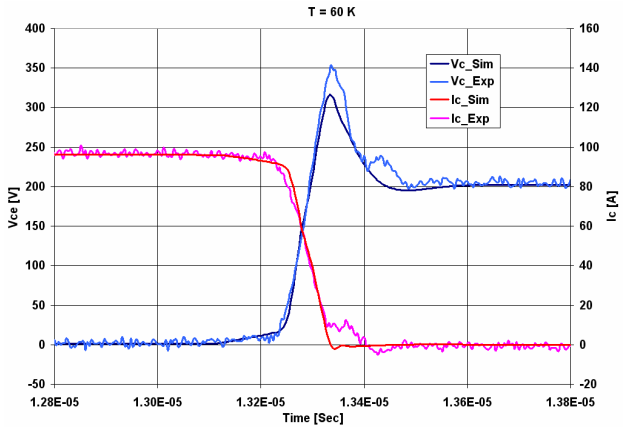

Figure 13: Comparison of simulation and experimental turn-off waveforms at 60 K. The current waveform shows the actual IGBT current without the snubber current.

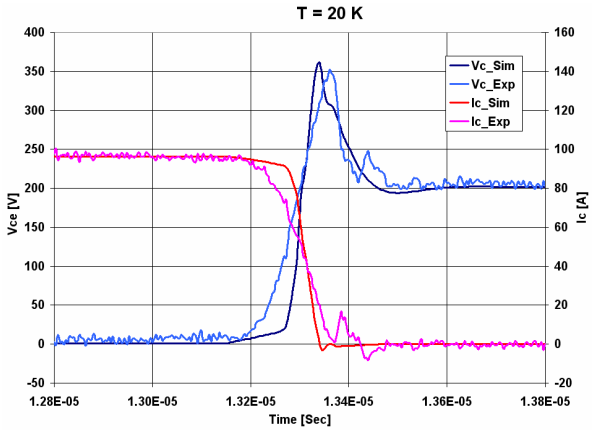

Figure 14: Comparison of simulation and experimental turn-off waveforms at 20 K. The current waveform shows the actual IGBT current without the snubber current.

Figure 13 and 14 show a comparison of simulation and experimental results at 60 K and 20 K, respectively. Collector-emitter voltage and collector current waveforms are compared. Since in the experiment only the resistive load current is measured, which is the sum of the IGBT and snubber current, the actual IGBT current is extrapolated from the load current and the IGBT collector-emitter voltage.

VI. Discussion

The mismatch between experimental and simulated data is currently under investigation. It can be at least partly attributed to the inaccurate representation of the silicon parameters at very low temperature.

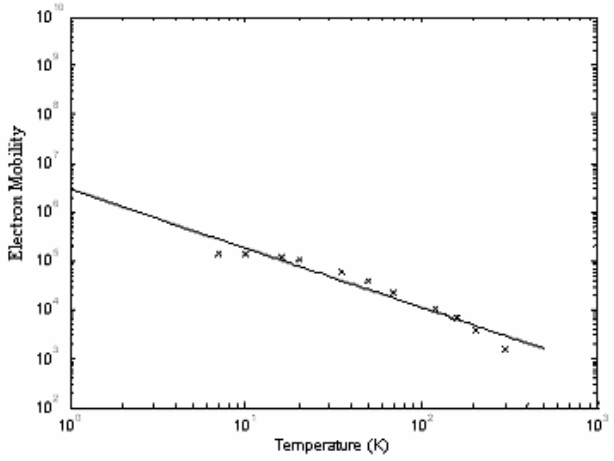

Figure 15: Electron mobility versus temperature. Experimental results are crosses and equation (3) is the continuous line

Unfortunately, limited data is available for silicon parameters at deep cryogenic temperatures. For example, Figure 15 shows the mobility data used in [9] to extract the electron mobility temperature dependence given by (3). The experimental mobility data tend to flatten at very low temperatures, while the mobility values given by (3) do not. Hence relation (3) may overestimate the mobility at low temperature resulting in a faster transition.

$$\mu_e = 2.92\times10^3\left(\frac{T}{300}\right)^{-1.21} \quad (3)$$

It is known that modeling of IGBTs below 100 K requires careful consideration of the material parameter relationships and their dependencies on temperature. The parameters of special interest include the density-of-states effective-masses for electrons and holes, the energy bandgap, the resulting intrinsic carrier concentration, the hole and electron mobilities, and the high-level carrier lifetime. Extrapolation of commonly used relationships for temperature dependencies becomes inadequate below 200 K. This is primarily due to the fact that the original temperature relationships were based on data obtained at 300 K or above. This necessitated a re-examination of the low-temperature data and creation of corrected relationships for all these parameters and quantities as previously reported [6]. There remain unknown interactions of effects that have not been adequately captured in the present model for operating temperatures below 20 K.

VII. CONCLUSIONS

In this work experimental data relative to the resistive turn off of IGBTs at deep cryogenic temperatures has been presented. Seven different devices from different manufacturers were extensively tested, showing fairly consistent behavior as a function of temperature. The Palmer-Leturcq IGBT model has been modified to extend its validity to deep cryogenic temperatures and its accuracy has been successfully verified for temperatures as low as 20 K by comparison with experimental waveforms.

VIII. ACKNOWLEDGMENTS

This work was supported by the U.S. Office of Naval Research under Grants N00014-02-1-0623 and N00014-03-1-0434

IX. REFERENCES

[1] V.A.K. Temple and F.W. Holroid "Feasibility study for low-temperature Thyristor operation", Power electronics Laboratory, Corporate Research and Development, Schenectady NY, n.86CRD220, Dec. 1986

[2] C.V. Godbold, J.L. Hudgins, C. Brown, W.M. Portnoy, "Temperature variation effects in MCTs, IGBTs and BMFETs" Power Electronics Specialists Conference, 1993. PESC '93 Record., 24th Annual IEEE , 20-24 June 1993 Page(s): 93 -98

[3] B. Lengler, "Semiconductor devices suitable for use in cryogenic environments" Cryogenics, Vol. 14, n. 8, Aug. 1974, pp 439-447

[4] J.F. Karner, H.W. Lorenzen, W. Rehm, "Semiconductors at low temperature", EPE Firenze, 1991

[5] F. Rosenbauer, H.W. Lorenzen, "Behavior of IGBT modules in the temperature range from 5 to 300K", Cryogenics engineering conference, Columbus, OH July 1995

[6] A. Caiafa, X. Wang, J.L. Hudgins, E. Santi, P. Palmer, "Cryogenic study and modeling of IGBT's" Power Electronics Specialists Conference, 2003. PESC 03. 2003 IEEE 34th Annual , Volume: 4 , 2003 15 – 19 June 2003 Page(s): 1897 -1903;

[7] S. Kolluri**, "**Application of distributed superconducting magnetic energy storage system (D-SMES) in the entergy system to improve voltage stability", Power Engineering Society Winter Meeting, 2002. IEEE , Volume: 2 , 27-31 Jan. 2002 Page(s): 838 -841 vol.2

[8] A. Caiafa, A. Snezhko, J. L. Hudgins, E. Santi, and R. Prozorov" IGBT operation at cryogenic temperatures: Non-Punch-Through and Punch-through comparison" " Power Electronics Specialists Conference, 2004. PESC 04. 2004 IEEE 35th Annual , Volume: X , 2004 20 – 25 June 2004.

[9] C. Jacoboni, C. Canali, G. Ottaviani, and A.A. Quaranta, "A review of some charge transport properties of silicon," *Solid-State Elec.*, vol. 20, pp. 77-89, 1977.

[10] P. Norton, T. Braggins, and H. Levinstein, *Phys. Rev.*, vol. B8, p. 5632, 1973.

[11] P.R. Palmer, J.C. Joyce, P.Y. Eng, J.L. Hudgins, E. Santi, and R. Dougal, "Circuit simulator models for the diode and IGBT with full temperature dependent features," IEEE PESC Rec., pp. 470-476, June 2001.

[12] Leturcq, Berraies, Debrie, Gillet, Kallala and Massol, "Bipolar semiconductor device models for computer-aided design in power electronics," 6th European Conference on Power Electronics, vol. 2, p. 84, Sept. 1995.

[13] X. Kang, A. Caiafa, E. Santi, J.L. Hudgins, and P.R. Palmer, "Parameter extraction for a power diode circuit simulator model including temperature dependent effects," IEEE APEC Rec., pp. 452-458, March 2002.

[14] X. Kang, A. Caiafa, E. Santi, J.L. Hudgins, and P.R. Palmer, "Low temperature characterization and modeling of IGBTs," IEEE PESC Rec., pp. , June 2002.

[15] X. Kang, A. Caiafa, E. Santi, J.L. Hudgins, and P.R. Palmer, "Characterization and modeling of high-voltage field-stop IGBTs," IEEE IAS Ann. Mtg. Rec., pp. , October 2002.